Solvent effects on catalytic activity and selectivity in amine-catalyzed D-fructose isomerization

Peter Drabo[a], Matthias Fischer[a], Meike Emondts[b], Jegor Hamm[a], Mats Engelke[a], Marc Simonis[a], Long Qi[c], Susannah L. Scott[d], Regina Palkovits[a], and Irina Delidovich[e*]*

[a]Chair of Heterogeneous Catalysis and Chemical Technology, Institute for Technical and Macromolecular Chemistry, RWTH Aachen University, Worringerweg 2, 52074 Aachen, Germany

[b]DWI - Leibniz Institute for Interactive Materials, Forckenbeckstr. 50, 52074 Aachen, Germany

[c]U.S. Department of Energy, Ames Laboratory, Iowa State University, Ames, Iowa 50011, United States

[d]Department of Chemical Engineering, University of California, Santa Barbara, California 93106, United States

[e]Institute of Chemical, Environmental and Bioscience Engineering, TU Wien, Getreidemarkt 9, 1060 Vienna, Austria

*delidovich@itmc.rwth-aachen.de; *palkovits@itmc.rwth-aachen

Abstract

Rational catalyst design and optimal solvent selection are key to advancing biorefining. Here, we explored the organocatalytic isomerization of D-fructose to a valuable rare monosaccharide, D-allulose, as a function of solvent. The isomerization of D-fructose to D-allulose competes with its isomerization to D-glucose, and sugar degradation. In both water and DMF, the catalytic activity of amines towards D-fructose is correlated with their basicity. Solvents impact the selectivity significantly by altering the tautomeric distribution of D-fructose. Our results suggest that the furanose tautomer of D-fructose is isomerized to D-allulose, and the fractional abundance of this tautomer increases as follows: water < MeOH < DMF ≈ DMF. Reaction rates are also higher in aprotic than in protic solvents, because …. The best D-allulose yield, 14 %, was obtained in DMF with 1,5,7-triazabicyclo[4.4.0]dec-5-ene (TBD) as the catalyst. The reaction kinetics and mechanism were explored using *operando* NMR spectroscopy, which showed that ….

Keywords: isomerization, D-fructose, D-allulose, D-glucose, amine, solvent effect, NMR

1

1. Introduction

D-allulose (also called D-psicose) is a rare monosaccharide of considerable industrial interest, particularly in the food industry where it serves as a low calorie sweetener [1, 2]. As a C3 epimer of D-fructose, D-allulose exhibits nutritional properties similar to common table sugar but with additional health benefits [1-3], such as a low glycemic response [4, 5], anti-inflammatory, neuroprotective and blood glucose suppressive effects [6]. In addition, their high chiral purity makes saccharides attractive as starting materials in organic synthesis. Saccharides have traditionally been used in the synthesis of fine chemicals [7, 8], but recent studies suggest they have potential in the production of some bulk chemicals as well [9-12]. For example, D-allulose was reported to be the most effective starting monosaccharide for making furanics by dehydration in methanol, resulting in higher yields than D-fructose, L-sorbose, or D-tagatose [5, 13].

D-allulose was discovered in small amounts as a nonfermentable constituent of cane molasses (where it as presumably formed by the Lobry de Bruyn Alberda van Ekenstein transformation [14-18]). It is also found in wheat or *Itea* plants [19-21]. Industrial production of D-allulose proceeds from readily accessible D-fructose via a biotechnology route. The use of enzymes ensures high selectivity to D-allulose, but comes with the drawbacks of high cost and low thermal stability for the enzymes [22]. Some of the reported chemical routes to D-allulose include chain extension of D-ribose *via* a cyanohydrine reaction [23] or reaction with diazomethane [24], aldol

addition [25] of protected or unprotected [26] C3 saccharides, and selective oxidation of protected D-fructose followed by reduction of an intermediate [27]. Synthetic schemes with their corresponding D-allulose yields are shown in Fig. 1S (see the electronic supplementary information, ESI). Costly substrates, numerous protection-deprotection steps, and/or long reaction times make these methods unattractive for large-scale production of D-allulose.

Isomerization of readily-available monosaccharides is a more attractive and atom-efficient method for D-allulose synthesis. Starting from D-glucose gives D-allulose in low yields of 0.2 to 5 % [28-32]. The transformation takes place *via* isomerization of D-glucose to D-fructose, followed by epimerization of the latter to D-allulose. Base-catalyzed isomerization of D-fructose in the aqueous phase gives rise to D-allulose in only slightly improved yields of 6-8 % [31-33]. These low yields can be explained by the low stability of D-allulose under the reaction conditions, as well as co-production of D-glucose and D-mannose (Fig. 1). Interestingly, higher yields of D-allulose (up to 10-12%) were reported for D-fructose isomerization in organic solvents such as ethanol [34], methanol [14, 35, 36], or pyridine [14]. To the best of our knowledge, the origin of this solvent effect has not been explained. In general, amine-catalyzed D-fructose isomerization has attracted much less attention compared to that of D-glucose [30, 37-45]. For the latter, the role of the amine structure in structure-activity [42] and structure-selectivity [43, 44] correlations have been reported. In addition,

the role of solvent on base-catalyzed isomerization of D-glucose to D-fructose has been described [46-49].

In this work, we systematically explored the catalytic isomerization of D-fructose in water, methanol, DMSO, and DMF in the presence of various amines as organocatalysts. *Ex situ* and *operando* NMR studies provide insight into the catalytic transformations of D-fructose.

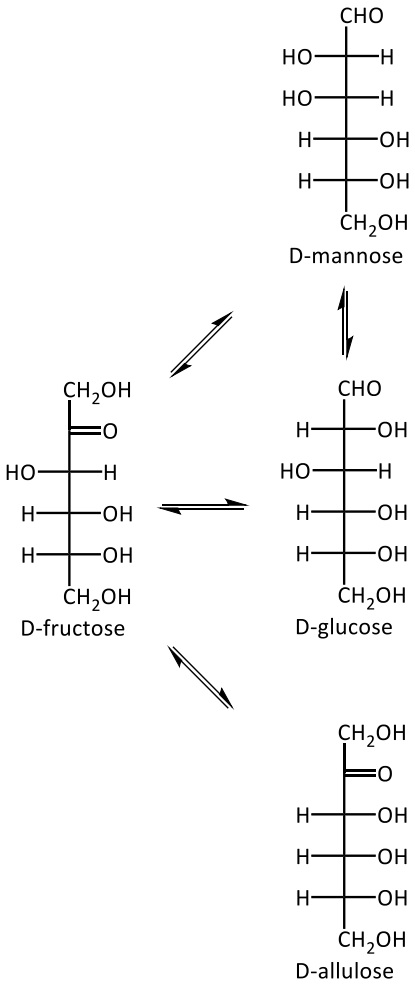

Figure 1. Simplified reaction network for D-fructose isomerization.

2. Experimental Section

2.1. Chemicals

All chemicals were used as received, without further purification. D-fructose (> 99.5 %), ethylene diamine (99.5 %), morpholine (> 99 %), sodium hydrogen carbonate (> 99 %), and triethylamine (99.5 %) were obtained from Carl Roth. D-glucose (Ph. Eur.), sulfuric acid (98 %), dimethyl sulfoxide (> 99 %), and *N,N,N',N'*-tetramethylguanidine (TMG, > 99 %) were purchased from Merck. 1,5,7-Triazabicyclo[4.4.0]dec-5-ene (TBD, 98 %), 1,5-diazabicyclo[4.3.0]non-5-ene (DBU, 98 %), [1-^{13}C]-D-glucose, Amberlyst® 15 in H^+-form, Dowex66® free base, and pyrrolidine were supplied by Sigma-Aldrich. 1-(3-aminopropyl)imidazole (API, 98 %) and dicyclohexylamine (DCHA, 98 %) were obtained from Alfa Aesar. 7-Methyl-1,5,7-triazabicyclo-[4.4.0]dec-5-ene (MTBD, > 95 %), 1,8-diazabicyclo[5.4.0]-7-undecene (DBU, > 98 %), *N*-ethylbutylamine (> 99 %) and dimethyl sulfoxide-d_6 (DMSO, 99.9 at% D) were purchased from TCI. Acetone (99.9 %) and methanol (99.9 %) were obtained from Chemsolute. Piperazine (99 %) was acquired from abcr. *n*-Tetradecane (99.5 %) was purchased from J&K. *N,N*-dimethylformamide (DMF) was bought from ITW Reagents. [2-^{13}C]-D-fructose (99 %) and [U-^{13}C6]-D-fructose (99%) were obtained from Cambridge Isotopes. Deuterium oxide (99.95 %), methanol-d_4 (99.8 %) and *N,N*-dimethyl-formamide-d_7 (99.5 %) were acquired from Deutero. D-allulose (> 98 %) was generously provided by SAVANNA Ingredients GmbH. All solutions were prepared in completely desalinated water.

2.2. Isomerization reaction

Isomerization of D-fructose was conducted in Ace pressure tubes (volume 9 mL), each equipped with a stirring bar. Stirring was conducted at 500 rpm. Typically, the pressure tubes were charged with 0.00166, 0.00333, or 0.00495 mmol D-fructose, an appropriate amount of catalyst, and 5.4 mL solvent. The pressure tubes were placed in a preheated oil bath (usually 60 or 80 °C). After the desired reaction time (up to 4 h), the pressure tubes were removed from the oil bath and the reaction was quenched by cooling in an ice bath.

2.3.Analysis of product mixtures

In general, analyses were performed as described previously [31]. Prior to analysis, samples were diluted 10-fold with distilled water and treated with two ion-exchange resins at room temperature to remove ionic species. Typically, Amberlyst®15 (H^+-form, 400 mg) was added to the diluted solution (10 mL) and the mixture was shaken for 0.5 h using a LAUDA Varioshake device. This ion-exchange resin was separated by filtration using polyamide syringe filters (CHROMAFIL PA, medium polar, 0.25 μm), then the solution was shaken with Dowex66® free base (1000 mg) for 1 h. The treatment with the ion-exchange resins was performed twice.

Quantification of organic products was performed by gas chromatography. Sugars were first transformed to their isopropylidene derivatives, following a modification of

a literature procedure [50]. First, aliquots of 1 mL were removed from each sample, frozen in liquid N_2, then dried in a vacuum desiccator. *n*-Tetradecane was added to the dry samples as an internal standard. The samples were shaken with H_2SO_4 (3 wt% in acetone, 2.5 mL) for 2.5 h at room temperature using a vortex shaker, then neutralized by shaking with $NaHCO_3$ for 1 h. The solid was filtered and analysis of the supernatant was performed using a HP 6890 gas chromatograph, equipped with a Machery-Nagel Optima 17-MS column (30 m x 0.25 μm) and an FID detector. The oven temperature was ramped from 80 to 250 °C at 12 °C·min^{-1}. Concentrations of the monosaccharides were calculated using the peak areas of the derivatives, referenced to *n*-tetradecane as an internal standard. The *n*-tetradecane signal eluted at 6.3 min, while D-allulose eluted at 9.3 min. Signals with retention times of 10.6 and 11.1 min corresponded to D-glucose and D-mannose, respectively. D-fructose showed two signals at 10.1 and 10.7 min, and its concentration was calculated by combining the areas of both peaks.

2.4. NMR measurements

Typically, the ^{13}C-labeled saccharide (D-fructose or D-glucose, 0.06-0.08 mmol) was dissolved in a deuterated solvent (D_2O, methanol-d_4, DMSO-d_6, or DMF-d_7, 0.5-0.6 mL). Experiments with unlabelled saccharides used larger amounts (typically, 0.2 mmol). Samples containing a saccharide and TBD were prepared with cooled D_2O (1 °C) or cooled DMF (-20 °C), and stored on ice upon measurement.

NMR spectra were recorded on a Bruker AV III 300 MHz, a Bruker AV III 400 MHz, a Bruker AV NEO 600 MHz or a Bruker AV NEO 500 MHz instrument. Quantitative ^{13}C NMR spectra were recorded using inverse-gated ^{1}H decoupling, a 90 ° pulse, and a recycle delay of 60 s. Kinetic experiments were conducted using power-gated ^{1}H decoupling, a 30 ° pulse, and a recycle delay of 2 s.

3. Results and discussion

3.1. Amine-catalyzed isomerization of D-fructose in water

The isomerization of D-fructose was studied in presence of various organic bases: morpholine (pK_a 8.4), 1-(3-aminopropyl)imidazole (API, pK_a 9.6), piperazine (pK_a 9.8), dicyclohexylamine (DCHA, pK_a 10.4), *N*-ethylbutylamine (pK_a 10.7), ethylenediamine (pK_a 10.8), triethylamine (TEA, pK_a 10.8), pyrrolidine (pK_a 11.3), tetramethylguanidine (TMG, pK_a 13.6), and 1,5,7-triazabicyclo[4.4.0]dec-5-en (TBD, pK_a 14.5). Here, pK_a refers to the acidity constant of the conjugate acid of the amine. Fig. 2 shows the structures of each of the primary, secondary, and tertiary amines. Isomerization was conducted at 80 °C, since this temperature allowed the recording of time-resolved concentration profiles on a convenient time scale for all of the amines tested as catalysts. During D-fructose conversion, D-allulose, D-glucose, and D-mannose were all observed by X. For each of the amine catalysts, aqueous-phase transformation of D-fructose resulted preferentially in the formation of D-glucose, with D-allulose and D-mannose being obtained in lower amounts. Thus, D-fructose

was converted to D-glucose at up to 28 % yield, while D-allulose and D-mannose yields were limited to 7 and 6%, respectively. These observations are in line with previous reports of aqueous-phase isomerization of D-fructose in the presence of various inorganic bases, including NaOH, $Ca(OH)_2$, and alkaline earth metal(hydr)oxides [14, 31, 32].

Interestingly, all of the amine catalysts tests show comparable selectivity-conversion plots (ESI Figure S2). The base-catalyzed isomerization of saccharides was previously reported to exhibit an induction period (Fig S2) [31, 51-54]. It was explained as the time needed for accumulate the enediolate anion before it reaches its steady-state concentration [51]. Selectivity for D-allulose reached a maximum after the induction period ended. At higher D-fructose conversions, the selectivity for D-allulose decreases due to the degradation of this highly reactive monosaccharide [29, 33]. Such degradation reactions give rise to acids such as lactic and glycolic acids [31], and/or oligomeric by-products [29, 31, 38, 55, 56], resulting in a mass balance below 100 % (ESI Figure S3).

We observed similar selectivities toward D-glucose, D-allulose, and D-mannose in the presence of all applied catalysts (Figure 3). While the highest selectivity towards D-glucose was in the range 33-43%, selectivities towards D-allulose (8-13) % and D-mannose (6-9) % were significantly lower.

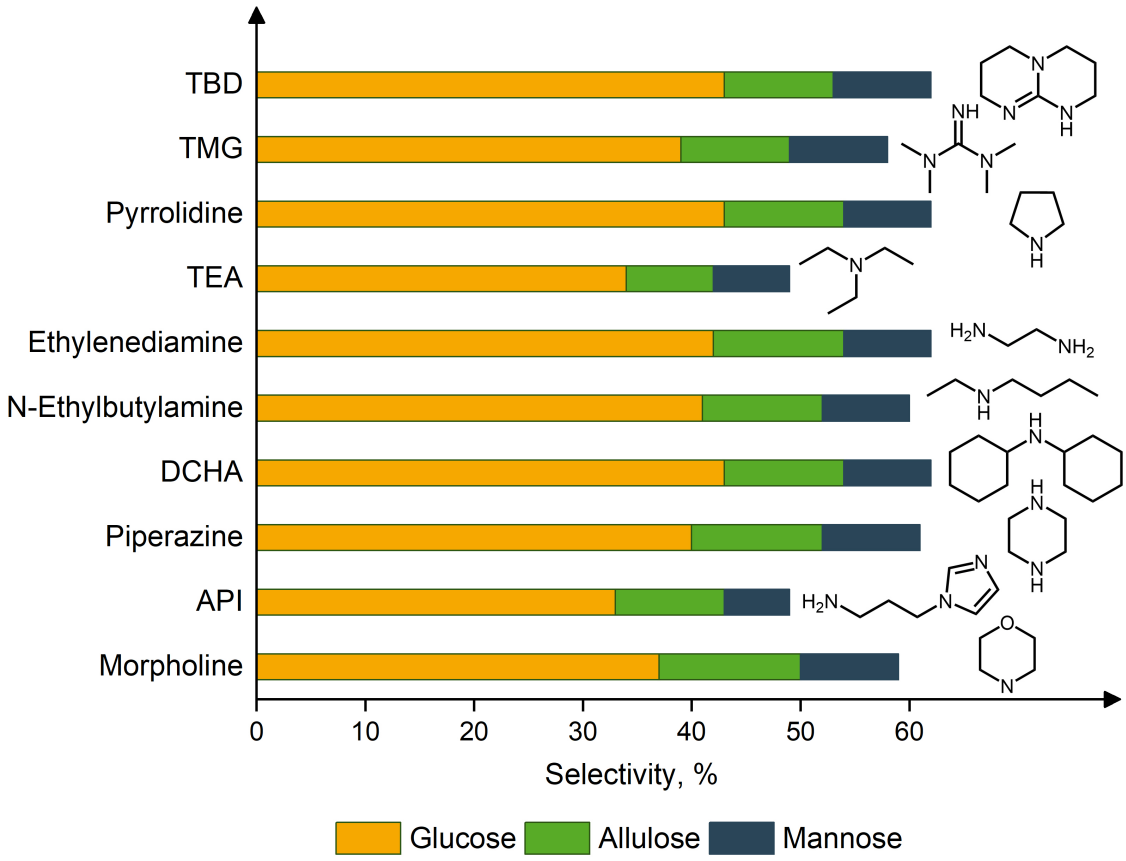

Figure 2. Results of D-fructose isomerization catalyzed by amines in aqueous solution. Reaction conditions: 80 °C, 4 mL H_2O, 0.0022 mol D-fructose, 0.00025 mol catalyst, 0-240 min.

Similar selectivities in the presence of the various amines point to the same catalytically active species, namely, OH^- generated via eq 1.

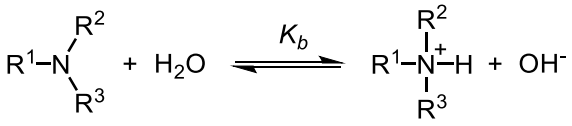

(1)

where the thermodynamic basicity constant K_b can be expressed as $K_b = [NR_1R_2R_3H^+][OH^-]/[NR_1R_2R_3]$. Carraher *et al.* also concluded that catalysis by OH^- was responsible for the aqueous-phase D-glucose-D-fructose isomerization, based on the similar product selectivity and activation energy in the presence of both TEA and NaOH [38]. The initial isomerization rate of D-fructose, r_0, can be expressed by eq 2:

$$r_0 = k_{\text{app}} \frac{K_{\text{Fru}}[OH^-]}{1 + K_{\text{Fru}}[OH^-]} C_{\text{Fru}} \quad (2)$$

where k_{app} refers to the apparent pH-independent rate constant, K_{Fru} denotes the thermodynamic ionization constant of D-fructose (13.8 at 80 °C [32]), and C_{Fru} is the initial concentration of D-fructose. The hydroxide concentration is $[OH^-] = \frac{\sqrt{K_b^2 + 4K_b C_{Amine}} - K_b}{2}$, where C_{Amine} is the amine concentration (here, 0.0625 M) and K_b is its basicity constant (eq 1). K_b can be calculated from the K_a value of the corresponding conjugate acid as $K_b = \frac{K_w}{K_a}$, where K_w is the autoionization constant of water (pK_w = 12.6 at 80 °C [32]). Figure 3 shows an excellent linear correlation between r_0 and $\frac{K_{Fru}[OH^-]}{1+K_{Fru}[OH^-]}$, supporting catalysis *via* OH^- generated by protonation of amines in water.

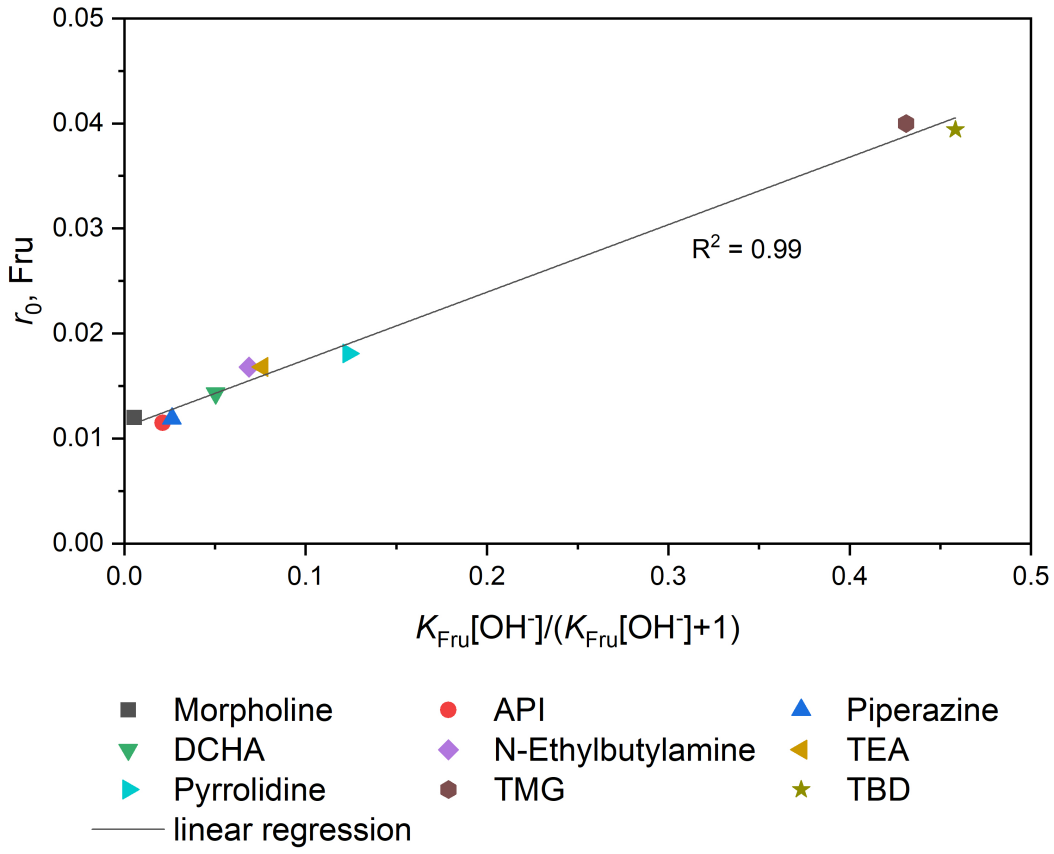

Figure 3. Initial rate of D-fructose consumption (r_0) as a function of [OH^-] for various amines in water. Reaction conditions: 80 °C, 4 mL H_2O, 0.0022 mol D-fructose, 0.00025 mol catalyst, 0-240 min.

3.2.Selectivity as a function of solvent and catalyst

The solvent-dependence of the selectivity was examined in MeOH, DMSO, and DMF, and compared to results obtained in water. TBD was chosen as the amine for this study, and reactions were conducted at 60 °C due to its higher catalytic activity in the organic solvents relative to water. It should be noted that D-fructose loadings as high as 15 wt.% in MeOH, DMSO, and DMF are apparently only possible in presence of amine, due to partial deprotonation of D-fructose by TBD.

Figure 4 shows the selectivities for the saccharide products at D-fructose conversions of 30-40%. The mass balance in the protic solvents water and methanol was significantly better than in the aprotic solvents DMSO and DMF (ESI Fig. S4-S11). In water and methanol, unidentified side-products accounted for 20-40%, whereas in DMSO and DMF the amount of side-products increased to 40-60%, based on ?. Increased formation of side-products in DMF compared to aqueous solution was confirmed by NMR (ESI Fig. S12). A change in the tautomer equilibria for the saccharides may explain the solvent-dependent stability of the saccharides. Table 1 shows the distribution of anomers for D-fructose, D-glucose, and D-allulose in various solvents. It is noteworthy that the fraction of the highly reactive open-chain forms, which are reported to be prone to degradation [57], increases significantly in DMSO and DMF compared to water and methanol, especially for D-fructose and D-allulose.

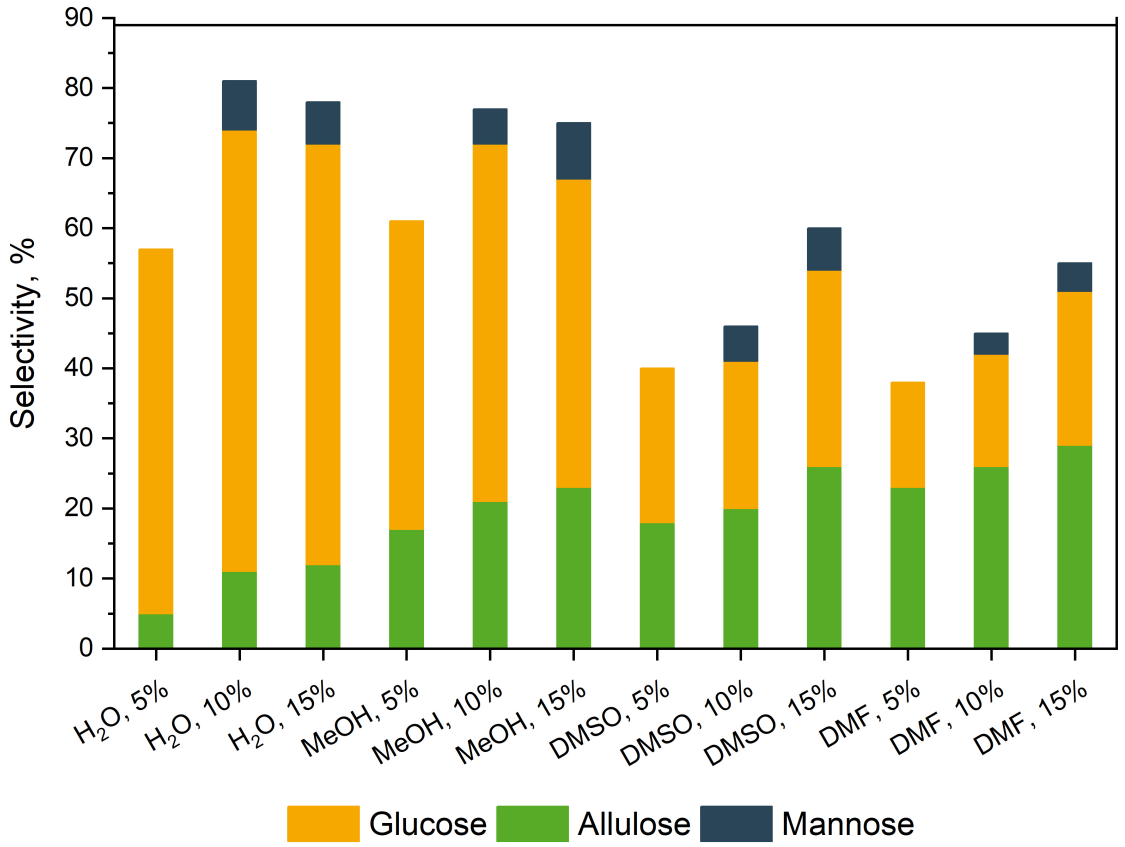

Figure 4. Selectivity in D-fructose isomerization catalyzed by TBD, as a function of solvent and initial D-fructose concentration. Reaction conditions: 60 °C, 5.4 mL solvent, 0.00165, 0.00333 or 0.00495 mol D-fructose, 0.00033 mol TBD, 0-240 min. Conversions between 30-40%.

Table 1. Tautomer equilibria for D-fructose, D-allulose and D-glucose in various solvents. Conditions: 25 °C, 0.6 mL solvent, 0.08 mmol [1-^{13}C]-D-glucose, 0.056-0.008 mmol [2-^{13}C]-D-fructose, or 0.20 mmol D-allulose (not labeled).

Entry	Saccharide	Solvent	Tautomeric form, %		
			Open chain	Furanoses (α/β)	Pyranoses (α/β)
1	D-fructose	D_2O	0.7	28.1 (20/80)	71.2 (4/96)

2		methanol-d_4	1.1	42.1 (25/75)	56.8 (7/93)
3		DMSO-d_6	3.0	67.4 (30/70)	29.5 (16/84)
4		DMF-d_7	2.4	64.4 (30/70)	33.2 (19/81)
5	D-allulose	D_2O	0.0	51.7 (71/29)	48.3 (51/49)
6		methanol-d_4	0.0	49.4 (81/19)	50.6 (45/55)
7		DMSO-d_6	3.8	48.2 (68/32)	48 (46/54)
8		DMF-d_7	1.0	48.0 (73/27)	51 (45/55)
9	D-glucose	D_2O	-	0.3 (67/33)	99.7 (38/62)
10		methanol-d_4	-	0.3 (0/100)	99.7 (51/49)
11		DMSO-d_6	-	0.5 (0/100)	99.5 (39/61)
12		DMF-d_7	-	0.8 (0/100)	99.2 (48/52)

Interestingly, the selectivity towards D-allulose depends on the D-fructose concentration (Figure 4). In water, the selectivity increases from 5 to 13% as the D-fructose concentration increases from 5 to 15 wt.%. Similar trends were observed in MeOH, DMSO, and DMF. The rise in D-allulose selectivity with increased initial D-fructose concentration can be explained by the changing substrate/catalyst ratio. Since the same TBD concentration was present for all reactions, 5 wt.% D-fructose corresponds to a substrate/catalyst ratio of 0.20. This ratio decreases to 0.066 when the D-fructose concentration is 15 wt.%. The higher catalyst-substrate ratio results in faster subsequent reactions, i.e., degradation of the saccharides. On the other hand, selectivity for D-glucose shows only a weak dependence on the initial substrate concentration. This is in line with a higher stability of D-glucose compared to D-

fructose [33], since the open-chain form of D-glucose was not detected even in aprotic solvents.

In sum, the isomerization of D-fructose to D-glucose and D-allulose occurs in competition with its degradation. Conditions disfavoring open-chain structures, and low concentrations of amine, limit side-reactions and improve the mass balance.

It is apparent from Figure 4 that the choice of solvent significantly affects the selectivity. Whereas the selectivity towards D-allulose is restricted to 13% in H_2O and 23% in MeOH, it rises to 26% in DMSO and 29% in DMF. Interestingly, the selectivity towards D-glucose shows the opposite trend. The tautomeric equilibria of the saccharides in Table 1 help to explain this observation. For D-fructose, the relative amounts of less energetically stable furanosides and more energetically stable pyranosides are solvent-dependent. In water, fructofuranosides represent *ca.* one-quarter of all fructose; in methanol, their share increases to *ca.* 40% and rises further to >60% in DMSO and DMF. Interestingly, the tautomeric equilibria of D-allulose and D-glucose are less influenced by solvent. Thus, the furanoside contribution is *ca.* 50% for D-allulose in all solvents, whereas D-glucose is present only in its pyranoside forms. Considering the high furanoside population for D-allulose along with the dominance of pyranosides for D-glucose, we hypothesize that D-fructose in its furanose forms isomerizes to D-allulose, whereas D-fructose in its pyranose forms gives rise to D-glucose. This hypothesis is based on the expectation that a smooth connection between substrate and product exists in the intrinsic reaction coordinate

[58]. Figure 5 illustrates these transformations, consistent with the generally accepted base-catalyzed mechanism for isomerization of saccharides [51]. Figure 6 reveals that the yields of D-allulose and D-glucose are indeed correlated with the relative amounts of furnanoses and pyranoses, respectively, explaining the observed effect of solvent on product selectivity. A similar solvent effect was previously reported for the dehydration of D-fructose to 5-hydroxymethylfurfural, which was more selective in solvents favoring fructofuranoside conformations [59-61]. It is worth noting that the tautomeric equilibria data in Table 2 were determined at room temperature. However, no significant changes in tautomeric distribution of D-fructose were detected at the reaction temperature (60 °C), although the contributions of the open-chain form and the furanosides increased somewhat, as expected [7].

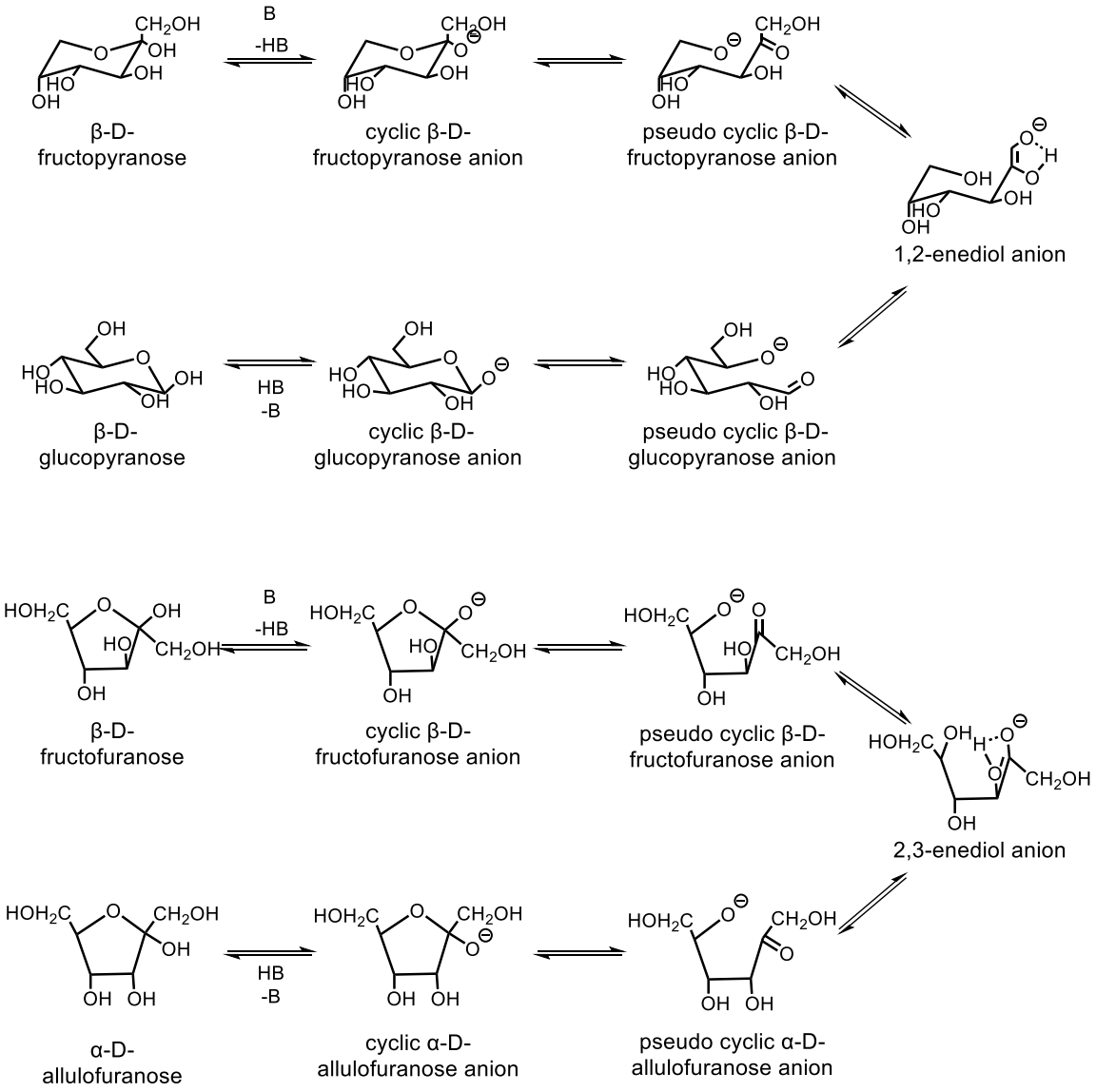

Figure 5. Proposed mechanism of D-fructopyranose isomerization to D-glucose (upper) and D-fructofuranose isomerization to D-allulose (lower).

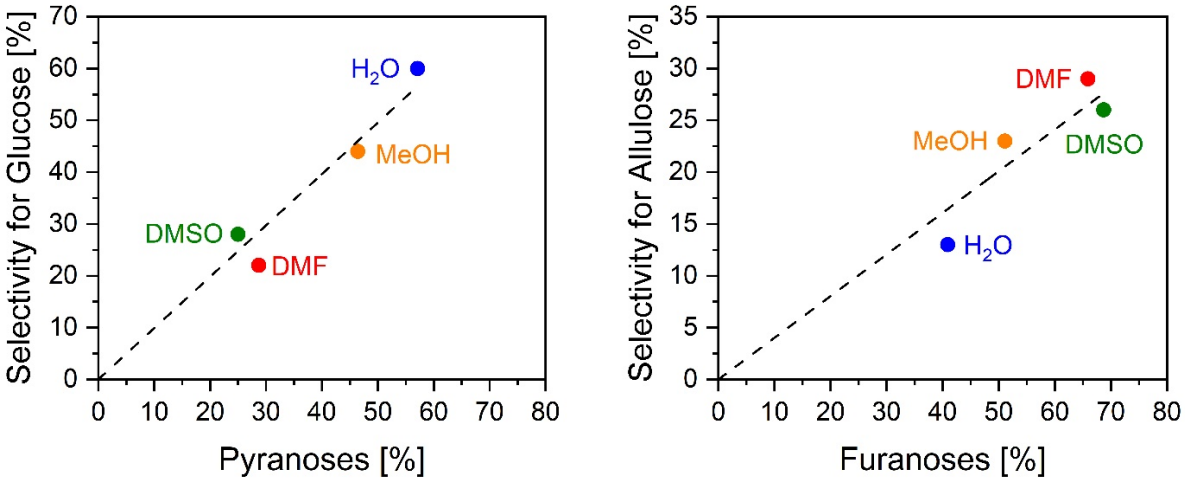

Figure 6: Selectivity for D-glucose (left) and D-allulose (right), depending on the tautomer contributions of fructopyranoses and fructofuranoses, respectively. Reaction conditions: 60 °C, 5.4 mL solvent, 0.00495 mol D-fructose, 0.00033 mol TBD, 0-240 min, conversions between 30-40%.

The influence of catalyst on selectivity was explored using various amidines (DBN and DBU) and guanidines (TMG, MTBD, and TBD) in DMF. Table 3 shows that selectivity for D-allulose (18-27 %) is higher than for D-glucose (9-12 %), with D-mannose formed in minor amounts. These selectivities are fairly independent of the amine structure, although the isomerization rate is correlated with amine basicity. The maximum yield of D-allulose is 14 %.

Table 2. Selectivity towards D-glucose, D-allulose, and D-mannose and their initial formation rates, during D-fructose isomerization catalyzed by amines. pK_a refers to

the acidity constant of the conjugate acid. Reaction conditions: 60 °C, 5.4 mL DMF, 0.00333 mol D-fructose, 0.00033 mol catalyst, 0-240 min.

Entry	Catalyst	Structure	pK_a[a]	Selectivity, %[b]			Initial formation rate, mmol·L^{-1}·min^{-1}		
				Glc	Allu	Man	Glc	Allu	Man
1	TMG	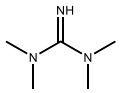	23.3[c]	12	21	0	0.2	0.3	0
2	DBN	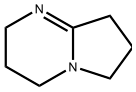	23.8[d]	10	23	0	0.2	0.4	0
3	DBU	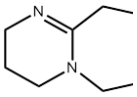	24.3[c]	9	18	0	0.3	0.5	0
4	MTBD	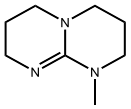	25.5[c]	12	19	2	1.0	1.6	0.2
5	TBD	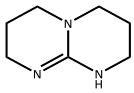	26.0[c]	12	27	0	3.8	6.3	0.4

[a] In MeCN; [b] For 30-40 % conversion; [c] pK$_a$ values from Ref. [62]; [c] pK$_a$ values from Ref. [63].

3.3. Solvent dependence of the reaction rate

Solvent selection clearly influences the isomerization rate. Comparison of the rates in different solvents was achieved using a kinetic solvent parameter (Equation 3) [64].

$$\sigma^P = log_{10} \frac{k^P_{org}}{k^P_{H2O}} \quad (3)$$

Here, P specifies one of the products, e.g., D-allulose, D-glucose, or D-mannose, while k_{org}^{P} is the rate constant for formation of that product in a particular organic solvent (MeOH, DMSO, or DMF). The product formation rate constant in water is designated k_{H2O}^{P}. If $\sigma^{P} > 0$, the specific product is formed faster than in pure water, while $\sigma^{P} < 0$ indicates the opposite. Rate constants for D-allulose formation were normalized by the initial D-fructofuranoside concentration, while those for D-glucose and D-mannose formation were normalized by the D-fructopyranoside concentration (ESI Equations S6-S8). We assumed that D-fructopyranosides isomerize to D-mannose, since the latter adopts mainly pyranoside structures [65].

Table 3 summarizes the kinetic solvent parameters for each of the solvents investigated here. The product-specific isomerization rates in methanol are very close to the rates in water, whereas they increase by factors of 2 to 8 in DMF and DMSO. This result may be due to better stabilization of the catalytically active species (hydroxide in water and, most likely, methoxide in methanol) compared to TBD in the polar aprotic solvents DMSO and DMF [66].

Table 3: Kinetic solvent parameters (σ^{P}) for isomerization of D-fructose to D-glucose, D-allulose, and D-mannose. Reaction conditions: 60 °C, 5.4 mL solvent, 0.0033 mol D-fructose, 0.00033 mol TBD, 0-240 min.

Entry	Solvent	σ^{Glc}	σ^{Allu}	σ^{Man}
1	H_2O	0	0	0

2	CH_3OH	-0.07	0.16	-0.08
3	DMSO	0.26	0.61	0.62
4	DMF	0.43	0.88	0.58

3.4. Operando NMR analysis of fructos isomerization

Operando NMR spectroscopy is a powerful tool enabling insights into the kinetics and mechanisms of saccharide transformations. The isomerization of [2-^{13}C]-D-fructose catalyzed by TBD was explored in DMF-d_7 and D_2O using *operando* ^{13}C NMR, Figure 7. In DMF, the signals of D-fructose and D-allulose are initially so broad that they are hardly observed during the first 2.5 h of the reaction. After 2.5 h, the catalyst deactivates (Figure S10) and the signals for fructo- and allulofuranoses sharpen. The corresponding pyranose signals also exhibit broadening, although to a lesser extent than for the furanose tautomers. This reflects the relative rates of tautomerization, which are reported to be significantly higher for furanoses than for pyranoses [67]. Formation of D-glucose and D-mannose, both of which are present in pyranose forms, is observed. Their signals are significantly sharper than those of D-fructose and D-allulose. The ^{13}C NMR line broadening observed for the different saccharides agrees well with the ^{1}H NMR data (Figure S13).

While this peak broadening hinders a fuller analysis of the *operando* NMR data, a semi-quantitative comparison of the results in DMF-d_7 and in D_2O suggests that the reaction is slower in aqueous medium, in agreement with the kinetic study described above. Interestingly, deuterium incorporation at the C2 position of D-glucose was

observed in D_2O, consistent with proton/deuteron exchange *via* an 1,2-enediol intermediate [16]. The 2-^{13}C peaks of glucose appear as triplets due to $^1J_{^{13}C^2H}$ coupling, while in the ^{1}H NMR spectrum, splitting of the peaks assigned to protons at the C1 position caused by $^3J_{HH}$ coupling disappears. In DMF-d_7, no deuterium incorporation was observed, as expected. Our current work focuses on optimization of NMR methods to obtain quantitative kinetic information .

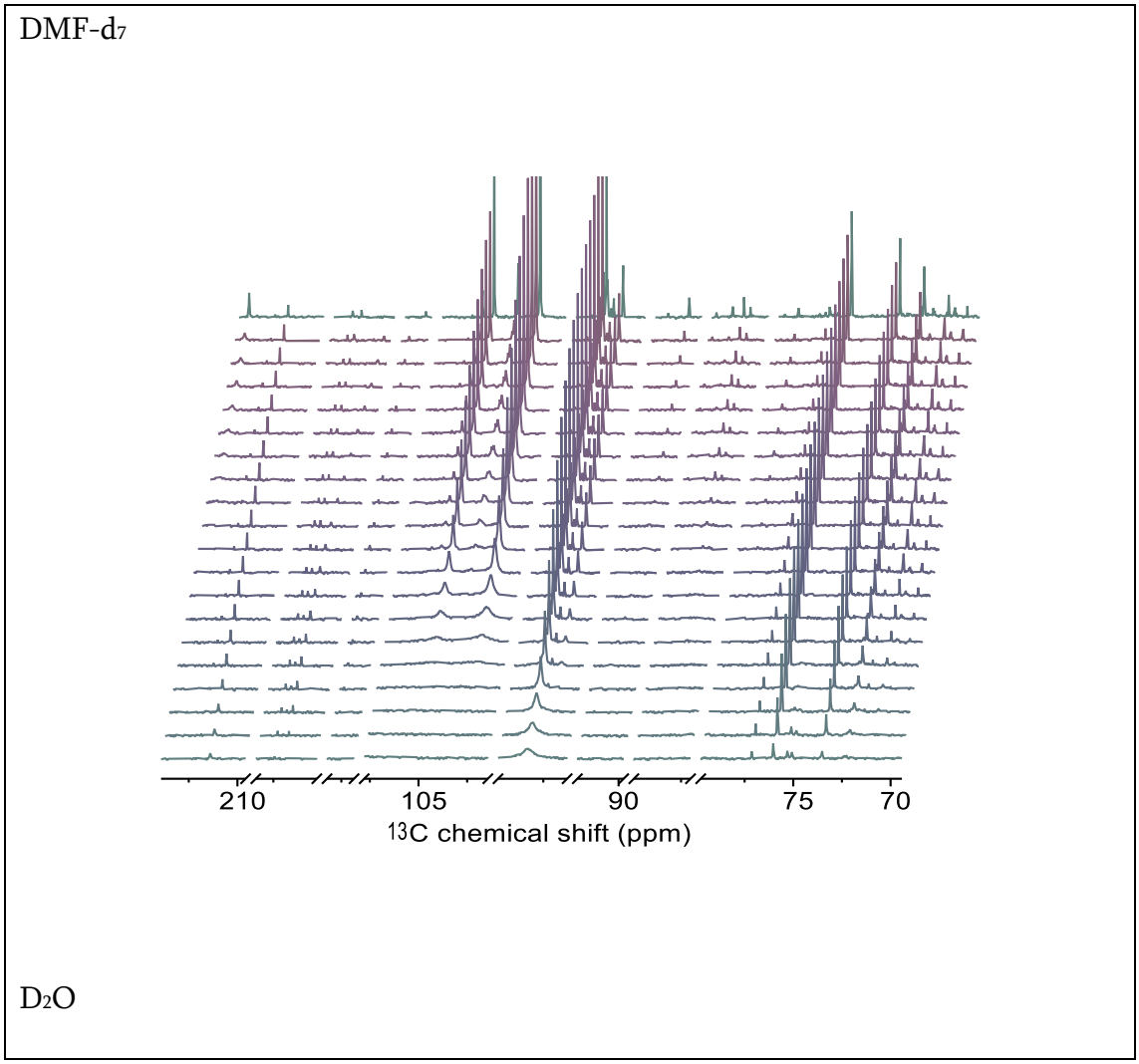

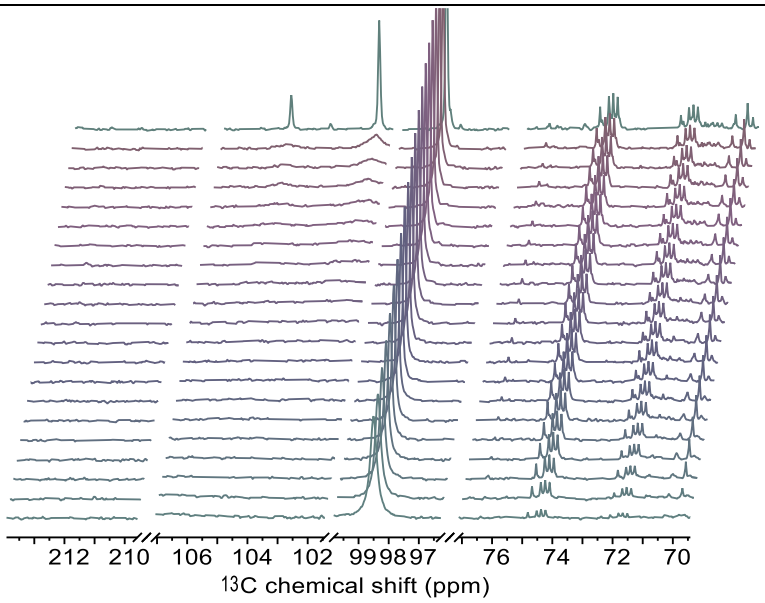

Figure 7. *Operando* NMR spectra showing fructose isomerization in DMF-d_7 (upper) and D_2O (lower). Reaction conditions: [2-^{13}C]-labelled D-fructose, 0.1 equiv. TBD as catalyst, 60 °C.

4. Conclusion

This work reveals the importance of two major contributions to the amine-catalyzed isomerization of D-fructose to D-allulose. The basicity of the amine is key in determining its catalytic activity. Interestingly, the solvent plays a dual role, regulating both *catalytic activity* – by stabilizing/destabilizing the catalytically active species – *and selectivity* – by influencing the tautomeric equilibrium of D-fructose. This understanding is essential for the rational development of methods for the chemocatalytic production of D-allulose.

ACKNOWLEDGMENT

We thank Carina Frantzen and Frederic Thilmany for their experimental contributions. We are grateful to Elke Biener, Hannelore Eschmann, and Heike Fickers-Boltz for performing the GC measurements. Furthermore, we would like to thank Ines Bachmann-Remy, Dr. Hongjun Zhou, Jerry Hu, and Oscar Nordness for their support during the NMR experiments. We gratefully acknowledge financial support by the BMEL (Bundesministerium für Ernährung und Landwirtschaft, Project 281A200316), by the DFG (Deutsche Forschungsgemeinschaft, Project 397970309), the US NSF (National Science Foundation, award 1805129) and by the thematic network *AcalNet* 2.0 for a travel grant. This work partly contributed to the Cluster of Excellence "The Fuel Science Center", which is funded by the Deutsche Forschungsgemeinschaft (DFG, German Research Foundation) under Germany's Excellence Strategy - Exzellenzcluster 2186 "The Fuel Science Center" (ID: 390919832).

5. References

[1] W. Mu, W. Zhang, Y. Feng, B. Jiang, L. Zhou, Recent advances on applications and biotechnological production of D-psicose, Appl. Microbiol. Biotechnol., 94 (2012) 1461-1467, 10.1007/s00253-012-4093-1.

[2] W. Zhang, S. Yu, T. Zhang, B. Jiang, W. Mu, Recent advances in d-allulose: Physiological functionalities, applications, and biological production, Trends in Food Science & Technology, 54 (2016) 127-137, https://doi.org/10.1016/j.tifs.2016.06.004.

[3] Y. Sun, S. Hayakawa, M. Ogawa, K. Izumori, Antioxidant properties of custard pudding dessert containing rare hexose, d-psicose, Food Control, 18 (2007) 220-227, https://doi.org/10.1016/j.foodcont.2005.09.019.

[4] S. Chattopadhyay, U. Raychaudhuri, R. Chakraborty, Artificial sweeteners - a review, Journal of food science and technology, 51 (2014) 611-621, https://doi.org/10.1007/s13197-011-0571-1.

[5] R.-J. van Putten, J.C. van der Waal, E. de Jong, H.J. Heeres, Reactivity studies in water on the acid-catalysed dehydration of psicose compared to other ketohexoses into 5-hydroxymethylfurfural, Carbohydr. Res., 446-447 (2017) 1-6, https://doi.org/10.1016/j.carres.2017.04.009.

[6] M.Y. Chung, D.K. Oh, K.W. Lee, Hypoglycemic health benefits of D-psicose, J. Agric. Food. Chem., 60 (2012) 863-869, https://doi.org/10.1021/jf204050w.

[7] F.W. Lichtenthaler, Towards improving the utility of ketoses as organic raw materials, Carbohydr. Res., 313 (1998) 69-89, https://doi.org/10.1016/S0008-6215(98)00222-5.

[8] V. Dimakos, M.S. Taylor, Site-Selective Functionalization of Hydroxyl Groups in Carbohydrate Derivatives, Chem. Rev., 118 (2018) 11457-11517, https://doi.org/10.1021/acs.chemrev.8b00442.

[9] I. Delidovich, K. Leonhard, R. Palkovits, Cellulose and hemicellulose valorisation: an integrated challenge of catalysis and reaction engineering, Energy Environ. Sci, 7 (2014) 2803, https://doi.org/10.1039/c4ee01067a.

[10] I. Delidovich, P.J. Hausoul, L. Deng, R. Pfützenreuter, M. Rose, R. Palkovits, Alternative Monomers Based on Lignocellulose and Their Use for Polymer Production, Chem. Rev., 116 (2015), https://doi.org/10.1021/acs.chemrev.5b00354.

[11] R.A. Sheldon, Chemicals from renewable biomass: A renaissance in carbohydrate chemistry, Curr. Opin. Green Sus. Chem., 14 (2018) 89-95, https://doi.org/10.1016/j.cogsc.2018.08.003.

[12] L. Ricciardi, W. Verboom, J.-P. Lange, J. Huskens, Production of furans from C5 and C6 sugars in the presence of polar organic solvents, Sustainable Energy & Fuels, 6 (2022) 11-28, https://doi.org/10.1039/d1se01572a.

[13] R.-J. van Putten, J.C. van der Waal, M. Harmse, H.H. van de Bovenkamp, E. de Jong, H.J. Heeres, A Comparative Study on the Reactivity of Various Ketohexoses to Furanics in Methanol, ChemSusChem, 9 (2016) 1827-1834, https://doi.org/10.1002/cssc.201600252.

[14] L.W. Doner, Isomerization of d-fructose by base: Liquid-chromatographic evaluation and the isolation of d-psicose, Carbohydr. Res., 70 (1979) 209-216, https://doi.org/10.1016/S0008-6215(00)87101-3.

[15] I. Delidovich, R. Palkovits, Catalytic Isomerization of Biomass-Derived Aldoses: A Review, ChemSusChem, 9 (2016) 547-561, https://doi.org/10.1002/cssc.201501577.

[16] H. Li, S. Yang, S. Saravanamurugan, A. Riisager, Glucose Isomerization by Enzymes and Chemo-catalysts: Status and Current Advances, ACS. Catal., 7 (2017) 3010-3029, https://doi.org/10.1021/acscatal.6b03625.

[17] R. Palkovits, I. Delidovich, Efficient utilization of renewable feedstocks: the role of catalysis and process design, Phil. Trans. R Soc. A, 376 (2018) 20170064, https://doi.org/10.1098/rsta.2017.0064.

[18] I. Delidovich, Recent progress in base-catalyzed isomerization of D-glucose into D-fructose, Curr. Opin. Green Sus. Chem., 27 (2021) 100414, https://doi.org/10.1016/j.cogsc.2020.100414.

[19] B.J. Ayers, J. Hollinshead, A.W. Saville, S. Nakagawa, I. Adachi, A. Kato, K. Izumori, B. Bartholomew, G.W.J. Fleet, R.J. Nash, Iteamine, the first alkaloid isolated from Itea virginica L. inflorescence, Phytochemistry, 100 (2014) 126-131, https://doi.org/10.1016/j.phytochem.2014.01.012.

[20] B.S. Miller, T. Swain, Chromatographic analyses of the free amino-acids, organic acids and sugars in wheat plant extracts, J. Sci. Food Agric., 11 (1960) 344-348, https://doi.org/10.1002/jsfa.2740110609.

[21] W.W. Binkley, The fate of cane juice simple sugars during molasses formation IV. Probable conversion of d-fructose to d-psicose, Int. Sugar J., 65 (1963) 105,

[22] A. Bosshart, N. Wagner, L. Lei, S. Panke, M. Bechtold, Highly Efficient Production of Rare Sugars D-Psicose and L-Tagatose by Two Engineered D-Tagatose Epimerases, Biotechnol. Bioeng., 113 (2016) 349-358, https://doi.org/10.1002/bit.25547.

[23] M. Steiger, T. Reichstein, d-Psicose, Helv. Chim. Acta, 19 (1936) 184-189, https://doi.org/10.1002/hlca.19360190129.

[24] M.L. Wolfrom, A. Thompson, E.F. Evans, The Action of Diazomethane upon Acyclic Sugar Derivatives. VII.1 D-Psicose2, J. Am. Che. Soc., 67 (1945) 1793-1797, https://doi.org/10.1021/ja01226a052.

[25] D. Enders, C. Grondal, Direkte organokatalytische De-novo-Synthese von Kohlenhydraten, Angew. Chem. , 117 (2005) 1235-1238, https://doi.org/10.1002/ange.200462428.

[26] A.L. Weber, Prebiotic sugar synthesis: Hexose and hydroxy acid synthesis from glyceraldehyde catalyzed by iron(III) hydroxide oxide, Journal of Molecular Evolution, 35 (1992) 1-6, https://doi.org/10.1007/BF00160255.

[27] E.J. McDonald, A new synthesis of d-psicose (d-ribo-hexulose), Carbohydr. Res., 5 (1967) 106-108, https://doi.org/10.1016/0008-6215(67)85014-6.

[28] L. Hough, J.K.N. Jones, E.L. Richards, The reaction of amino-compounds with sugars. Part II. The action of ammonia on glucose, maltose, and lactose, J. Chem. Soc. (Resumed), (1953) 2005-2009, https://doi.org/10.1039/JR9530002005.

[29] S.J. Angyal, The Lobry de Bruyn-Alberda van Ekenstein Transformation and Related Reactions, in: A.E. Stütz (Ed.) Glycoscience, Springer, Berlin, Heidelberg, 2001, pp. 1-14, https://doi.org/10.1007/3-540-44422-x_1.

[30] S. Kumar, S. Sharma, S.K. Kansal, S. Elumalai, Efficient Conversion of Glucose into Fructose via Extraction-Assisted Isomerization Catalyzed by Endogenous Polyamine Spermine in the Aqueous Phase, ACS Omega, 5 (2020) 2406-2418, 10.1021/acsomega.9b03918.

[31] P. Drabo, M. Fischer, V. Toussaint, F. Flecken, R. Palkovits, I. Delidovich, What are the catalytically active species for aqueous-phase isomerization of D-glucose into D-fructose in the presence of alkaline earth metal (hydr)oxides?, J. Catal., 402 (2021) 315-324, https://doi.org/10.1016/j.jcat.2021.08.036.

[32] M. Fischer, P. Drabo, I. Delidovich, Manuscript submitted, (2022),

[33] J.M. de Bruijn, A.P.G. Kieboom, H. van Bekkum, Alkaline degradation of monosaccharides V: Kinetics of the alkaline isomerization and degradation of monosaccharides, Rec. Trav. Chim. Pays Bas, 106 (1987) 35-43, https://doi.org/10.1002/recl.19871060201.

[34] R.J. Beveridge, M. Davis, J.L. Morris, N.J. Hoogenraad, The preparation of decagram quantities of d-psicose by the isomerization of d-fructose, and separation of the products on a calcium-ion cation-exchange resin, Carbohydr. Res., 101 (1982) 348-349, https://doi.org/10.1016/S0008-6215(00)81019-8.

[35] K. Heyns, H. Paulsen, H. Schroeder, Die umsetzung von ketohexosen mitsekundären aminosäuren und sekundärenaminen, Tetrahedron, 13 (1961) 247-257, https://doi.org/10.1016/S0040-4020(01)92218-5.

[36] S. Passeron, E. Recondo, Notes, J. Chem. Soc. (Resumed), (1965) 813-815, https://doi.org/10.1039/JR9650000786.

[37] C. Liu, J.M. Carraher, J.L. Swedberg, C.R. Herndon, C.N. Fleitman, J.-P. Tessonnier, Selective Base-Catalyzed Isomerization of Glucose to Fructose, ACS Catal., 4 (2014) 4295-4298, 10.1021/cs501197w.

[38] J.M. Carraher, C.N. Fleitman, J.-P. Tessonnier, Kinetic and Mechanistic Study of Glucose Isomerization Using Homogeneous Organic Brønsted Base Catalysts in Water, ACS Catal., 5 (2015) 3162-3173, https://doi.org/10.1021/acscatal.5b00316.

[39] Q. Yang, S. Zhou, T. Runge, Magnetically separable base catalysts for isomerization of glucose to fructose, J. Catal., 330 (2015) 474-484, https://doi.org/10.1016/j.jcat.2015.08.008.

[40] Q. Yang, W. Lan, T. Runge, Salt-Promoted Glucose Aqueous Isomerization Catalyzed by Heterogeneous Organic Base, ACS Sustain. Chem. Eng., 4 (2016) 4850-4858, https://doi.org/10.1021/acssuschemeng.6b01132.

[41] Q. Yang, T. Runge, Polyethylenimines as Homogeneous and Heterogeneous Catalysts for Glucose Isomerization, ACS Sustainable Chemistry & Engineering, 4 (2016) 6951-6961, 10.1021/acssuschemeng.6b01880.

[42] N. Deshpande, E.H. Cho, A.P. Spanos, L.-C. Lin, N.A. Brunelli, Tuning molecular structure of tertiary amine catalysts for glucose isomerization, J. Catal., 372 (2019) 119-127, https://doi.org/10.1016/j.jcat.2019.02.025.

[43] S.S. Chen, D.C.W. Tsang, J.-P. Tessonnier, Comparative investigation of homogeneous and heterogeneous Brønsted base catalysts for the isomerization of glucose to fructose in aqueous media, Appl. Catal. B: Environ, 261 (2020) 118126, https://doi.org/10.1016/j.apcatb.2019.118126.

[44] N. Zhang, X.-G. Meng, Y.-Y. Wu, H.-J. Song, H. Huang, F. Wang, J. Lv, Highly Selective Isomerization of Glucose into Fructose Catalyzed by a Mimic Glucose Isomerase, ChemCatChem, 11 (2019) 2355-2361, 10.1002/cctc.201900143.

[45] Q. Yang, M. Sherbahn, T. Runge, Basic Amino Acids as Green Catalysts for Isomerization of Glucose to Fructose in Water, ACS Sustainable Chemistry & Engineering, 4 (2016) 3526-3534, https://doi.org/10.1021/acssuschemeng.6b00587.

[46] M. Yabushita, N. Shibayama, K. Nakajima, A. Fukuoka, Selective Glucose-to-Fructose Isomerization in Ethanol Catalyzed by Hydrotalcites, ACS. Catal., 9 (2019) 2101-2109, https://doi.org/10.1021/acscatal.8b05145.

[47] P.P. Upare, A. Chamas, J.H. Lee, J.C. Kim, S.K. Kwak, Y.K. Hwang, D.W. Hwang, Highly Efficient Hydrotalcite/1-Butanol Catalytic System for the Production of the High-Yield Fructose Crystal from Glucose, ACS. Catal., 10 (2020) 1388-1396, https://doi.org/10.1021/acscatal.9b01650.

[48] P. Zhu, S. Meier, A. Riisager, Stannate-catalysed glucose-fructose isomerisation in alcohols, Catal. Sci. Technol., (2022), https://doi.org/10.1039/d2cy00901c.

[49] X. Du, A.W. Tricker, W. Yang, R. Katahira, W. Liu, T.T. Kwok, P. Gogoi, Y. Deng, Oxidative Catalytic Fractionation and Depolymerization of Lignin in a One-Pot Single-Catalyst System, ACS Sus. Chem. Eng., 9 (2021) 7719-7727, https://doi.org/10.1021/acssuschemeng.0c08448.

[50] D. Ekeberg, S. Morgenlie, Y. Stenstrøm, Aldose–ketose interconversion in pyridine in the presence of aluminium oxide, Carbohydr. Res., 342 (2007) 1992-1997, http://dx.doi.org/10.1016/j.carres.2007.05.033.

[51] G. De Wit, A.P.G. Kieboom, H. van Bekkum, Enolisation and isomerisation of monosaccharides in aqueous, alkaline solution, Carbohydr. Res., 74 (1979) 157-175, https://doi.org/10.1016/S0008-6215(00)84773-4.

[52] I.K.M. Yu, A. Hanif, D.C.W. Tsang, J. Shang, Z. Su, H. Song, Y.S. Ok, C.S. Poon, Tuneable functionalities in layered double hydroxide catalysts for thermochemical conversion of biomass-derived glucose to fructose, Chem. Eng. J., 383 (2020) 122914, https://doi.org/10.1016/j.cej.2019.122914.

[53] M.M. Antunes, A. Fernandes, D. Falcão, M. Pillinger, F. Ribeiro, A.A. Valente, Optimized preparation and regeneration of MFI type base catalysts for d-glucose isomerization in water, Catal. Sci. Technol., 10 (2020) 3232-3246, https://doi.org/10.1039/d0cy00188k.

[54] I. Delidovich, M.S. Gyngazova, N. Sánchez-Bastardo, J.P. Wohland, C. Hoppe, P. Drabo, Production of keto-pentoses via isomerization of aldo-pentoses catalyzed by phosphates and recovery of products by anionic extraction, Green Chem., 20 (2018) 724-734, https://doi.org/10.1039/C7GC03077K.

[55] I. Delidovich, R. Palkovits, Structure–performance correlations of Mg–Al hydrotalcite catalysts for the isomerization of glucose into fructose, J. Catal., 327 (2015) 1-9, http://dx.doi.org/10.1016/j.jcat.2015.04.012.

[56] J.M. de Bruijn, A.P.G. Kieboom, H. van Bekkum, Alkaline degradation of monosaccharides III. Influence of reaction parameters upon the final product composition, Rec. Trav. Chim. Pays Bas, 105 (1986) 176-183, https://doi.org/10.1002/recl.19861050603.

[57] X. Fu, Y. Hu, Y. Zhang, Y. Zhang, D. Tang, L. Zhu, C. Hu, Solvent Effects on Degradative Condensation Side Reactions of Fructose in Its Initial Conversion to 5-Hydroxymethylfurfural, ChemSusChem, 13 (2020) 501-512, 10.1002/cssc.201902309.

[58] M. Asakawa, A. Shrotri, H. Kobayashi, A. Fukuoka, Solvent basicity controlled deformylation for the formation of furfural from glucose and fructose, Green Chemistry, 21 (2019) 6146-6153, https://doi.org/10.1039/c9gc02600b.

[59] M.H. Tucker, R. Alamillo, A.J. Crisci, G.M. Gonzalez, S.L. Scott, J.A. Dumesic, Sustainable Solvent Systems for Use in Tandem Carbohydrate Dehydration Hydrogenation, ACS Sustainable Chemistry & Engineering, 1 (2013) 554-560, https://doi.org/10.1021/sc400044d.

[60] H. Kimura, M. Nakahara, N. Matubayasi, Solvent Effect on Pathways and Mechanisms for <scp>d</scp>-Fructose Conversion to 5-Hydroxymethyl-2-furaldehyde: In Situ ¹³C NMR Study, The Journal of Physical Chemistry A, 117 (2013) 2102-2113, https://doi.org/10.1021/jp312002h.

[61] G.S. Svenningsen, R. Kumar, C.E. Wyman, P. Christopher, Unifying Mechanistic Analysis of Factors Controlling Selectivity in Fructose Dehydration to

5-Hydroxymethylfurfural by Homogeneous Acid Catalysts in Aprotic Solvents, ACS. Catal., 8 (2018) 5591-5600, https://doi.org/10.1021/acscatal.8b01197.

[62] I. Kaljurand, A. Kütt, L. Sooväli, T. Rodima, V. Mäemets, I. Leito, I.A. Koppel, Extension of the Self-Consistent Spectrophotometric Basicity Scale in Acetonitrile to a Full Span of 28 pKa Units: Unification of Different Basicity Scales, The Journal of Organic Chemistry, 70 (2005) 1019-1028, 10.1021/jo048252w.

[63] T. Ishikawa, Guanidines in Organic Synthesis, in: Superbases for Organic Synthesis, 2009, pp. 93-143, 10.1002/9780470740859.ch4.

[64] T.W. Walker, A.K. Chew, H. Li, B. Demir, Z.C. Zhang, G.W. Huber, R.C. Van Lehn, J.A. Dumesic, Universal kinetic solvent effects in acid-catalyzed reactions of biomass-derived oxygenates, Energy & Environmental Science, 11 (2018) 617-628, 10.1039/c7ee03432f.

[65] J.B. Lambert, G. Lu, S.R. Singer, V.M. Kolb, Silicate Complexes of Sugars in Aqueous Solution, Journal of the American Chemical Society, 126 (2004) 9611-9625, https://doi.org/10.1021/ja031748v.

[66] J.J. Varghese, S.H. Mushrif, Origins of complex solvent effects on chemical reactivity and computational tools to investigate them: a review, Reaction Chemistry & Engineering, 4 (2019) 165-206, 10.1039/c8re00226f.

[67] J.R. Snyder, E.R. Johnston, A.S. Serianni, D-Talose anomerization: NMR methods to evaluate the reaction kinetics, J. Am. Chem. Soc., 111 (1989) 2681-2687, https://doi.org/10.1021/ja00189a050.

1